Real-time PMIRRAS studies of *in situ* growth of $C_{11}Eg_6OMe$ on gold and immersion effects†

Stefan Zorn,[a] Nathan Martin,[ab] Alexander Gerlach[a] and Frank Schreiber*[a]

Received 11th November 2009, Accepted 12th May 2010
DOI: 10.1039/b923691k

We studied the growth of self-assembling monolayers of $C_{11}Eg_6OMe$ on gold under aqueous conditions. With the help of polarisation modulation infrared reflection absorption spectroscopy (PMIRRAS) we monitored the evolution of characteristic absorption modes in the fingerprint region (1050–1500 cm^{-1}) during the later stages of the growth of the SAM. We observed a change from rather amorphous structure with mixed all-*trans* and helical conformation to an ordered structure with predominantly helical structure over time. Changes of mode positions, intensities and broadness can be described by a single exponential. In addition, we investigated the effect of hydration for SAMs with different degrees of crystallinity. To that end, we compared their spectra at certain ordering levels in contact with aqueous solution with the corresponding spectra in air. SAMs with a highly ordered crystalline structure in air show the same structure under aqueous conditions. However, SAMs which are still crystalline in air, but less perfect, show rather amorphous spectral features under aqueous conditions indicating a strong interaction with water. This implies that the ability of water to penetrate the EG moiety strongly depends on its structure which in turn is related *inter alia* to the surface coverage. Since the interaction with water plays an important role in the prevention of unspecific adsorption on oligo(ethylene glycols) this is important for its application. Our experiments also underline the importance of the *in situ* analysis of the film structure.

1. Introduction

Self-assembled monolayers (SAMs) containing ethylene glycol units gained tremendous importance in biotechnological and medical applications.[1–3] Prime and Whitesides[4,5] showed that not only *poly*-ethylene glycols are able to render surfaces resistant against unspecific protein adsorption but also short chained oligo-ethylene glycols (OEGs). They can also be used as a spacer for tethering various groups for specific binding of proteins[6] or DNA[7] and so be applicable for biosensors. They are also useful as a supporting layer of lipid films which are able to retain their crystalline-liquid structure due to the soft underlayer[8] which makes them a valuable tool in biotechnology.

Owing to their importance there has been extensive work in order to understand the underlying mechanisms of the protein resistance and the structural behaviour of OEGs. It was shown that OEGs with three ethylene glycol (EG) units have different conformations on Ag and Au substrates due to different lattice spacing which allows control of their protein resistance.[9] Theoretical work suggested that a perfect helical conformation is most favourable for SAMs with 6 EG units, but that small distortions increase the energy of the system only slightly.[10] With increasing temperature it is possible to change the structure of OEG SAMs with 6 EG units from a predominant helical conformation to an all-*trans* conformation.[11] Vanderah *et al.*[12] showed that the protein resistance of SAMs with 6 EG units depends on the surface coverage with its impact on the conformation and crystallinity of the SAM and concluded that perfect ordered helical SAMs with 6 EG units with full surface coverage are not completely resistant against protein adsorption (see also ref. 13) while such with about 80–90% surface coverage are. Generally there are many conflicting reports concerning the order and protein resistance of OEG SAMs, implying that the SAMs structure is very sensitive towards different preparation conditions *e.g.* regarding surfactant concentration and growth time.[12,14–16] A deeper understanding of the growth process may shed light on this and may lead to a higher reproducibility of SAM growth.

An important point in understanding the structural behaviour and protein resistant properties of OEG SAMs is also their interaction with the water molecules. In an *in situ* PMIRRAS study with OEG SAMs containing 3 EG units Skoda *et al.*[17] showed that there is a red-shift in the C–O–C stretching region of SAMs in solution with respect to spectra in air which indicates an interaction with water. Also sum frequency generation (SFG) studies showed that there is a distortion of the SAM structure of SAMs with 3 EG units[18] and 6 EG units[14] due to the interaction with water. Wang *et al.* reported that not only the upper EG units are affected but also interior ones and that their conformational freedom is increased by the interaction with water. Wang *et al.*[19] showed with density functional theory a possible explanation of this strong perturbation. In air perfect helical structures are most favourable

[a] *Institute for Applied Physics, Eberhard-Karls University of Tübingen, Auf der Morgenstelle 10, 72076 Tübingen, Germany. E-mail: frank.schreiber@uni-tuebingen.de*
[b] *Montana State University, Bozeman, Montana 59717, USA*
† Electronic supplementary information (ESI) available: experimental details, figure. See DOI: 10.1039/b923691k

and especially conformers with *gauche* rotations of opposite directions around neighbouring EG units are most unfavourable due to the capability of the formation of intramolecular hydrogen bonds. Based on the formation of intra- and intermolecular hydrogen bridge structures with water molecules, these conformers with *gauche* defects are in an aqueous environment more favourable than perfect helical structures. This leads to an amorphisation if water can penetrate the EG layer.[14,18]

For this study we have monitored the later stages of the growth of the (hexaethylene glycol) terminated thiol $HS(CH_2)_{11}(OCH_2CH_2)_6OMe$ (Eg_6OMe) in solution with PMIRRAS in real time. We were able to track the modes in the fingerprint region and observe a conformational change from mixed all-*trans* and helical OEG moieties to predominant helical ones. Further we will show the differences in conformation under aqueous conditions relative to in air conformation and the level of the change with respect to the surface coverage.

2. Experimental section

2.1 Sample preparation

We used gold coated glass slides as substrates (Arrandee). The slides were successively sonicated in MilliQ water (18.2 MΩ cm, Millipore) and ethanol (99.9%, Riedel de Haen), then dried in an argon stream, treated with ozone producing UV-light for 20 min and rinsed with MilliQ water. The cleaning treatment was done directly before each experiment. For the SAM growth we used a 1.25 mM solution of $C_{11}Eg_6OMe$ (Prochimia, Gdansk, Poland) in MilliQ water with 0.1 M NaF.

2.2 PMIRRAS measurements and data analysis

The setup has been described recently.[17,20,21] In short, we used a Vertex70 equipped with a PMA50 unit (Bruker, Ettlingen, Germany), 256 scans were co-added in the first 2 h of the growth process and 1024 in the subsequent time. The measurements were carried out with a homemade liquid cell,[17] ensuring a 1–2 μm thick solution layer in between the substrate and a BaF_2 half cylinder, we added NaF (0.1 M) to the solution, to enhance the stability of BaF_2. The thickness of the liquid layer is crucial for the quantitative analysis and was controlled by ellipsometry. Note that due to the small thickness of the liquid layer, which is necessary to measure a reasonable signal in the interesting spectral region close to a strong infrared absorption mode of water,[21] the measurements were made under non-flow conditions and so the absolute number of thiol molecules in solution is smaller compared to growth in bulk solution and is decreasing during the growth. However, since there are no changes in the setup necessary during the whole measurement, this method is well suited to reliably measure relative changes over time with a high level of stability.

The IR spectra were exported from OPUS (Bruker) and further processed in IgorPro (Wavemetrics). First, we made a baseline correction as described elsewhere.[21] Then we performed a multiple Gaussian fitting procedure to extract characteristics of the different infrared absorption modes regarding to area, width and position.

3. Results and discussion

3.1 Identification and significance of the vibrational modes

Before analysing their temporal evolution, we first explain the assignment and significance of the vibrational modes. We concentrate on the spectral range from approximately 1050 cm^{-1} to 1400 cm^{-1} (Fig. 1). This so-called 'fingerprint region' contains a number of absorption modes which are characteristic for the different conformations of the molecules in the SAM. A detailed assignment of the modes can be found in the literature.[9,22,23] A position of the C–O–C stretching mode at 1116 cm^{-1}, an ether CH_2 twisting mode at 1244 cm^{-1} and an ether wagging mode at 1348 cm^{-1} are indicating a helical structure of the OEG moiety of the SAM. In contrast, a C–O–C stretching mode at 1144 cm^{-1} and an ether wagging mode at 1325 cm^{-1}, which may be split, indicate an all-*trans* conformation of the OEG-SAM.[9] A broadening, attenuation and a blue-shift of the absorption modes and the coexistence of modes characteristic for both conformations in fairly equal parts indicate a rather amorphous structure instead of a crystalline one.[9,17]

The CH_3 rocking mode at about 1200 cm^{-1}, a feature from the CH_3 end-group of the OEG-SAM, seems to be rather independent of conformational changes and can be used as an indicator for the surface coverage of the SAM. The reason for this insensitivity to structural changes is supposed to be due to its large interaction with water molecules and the resulting random orientation in aqueous solution.[18] See Table 1 for a summary of the vibrational modes.

3.2 Evolution of the modes

Since mounting of our thin liquid-layer-cell takes roughly 2 minutes and a scan with reasonable signal-to-noise ratio another 4 minutes, the first spectrum taken by us corresponds

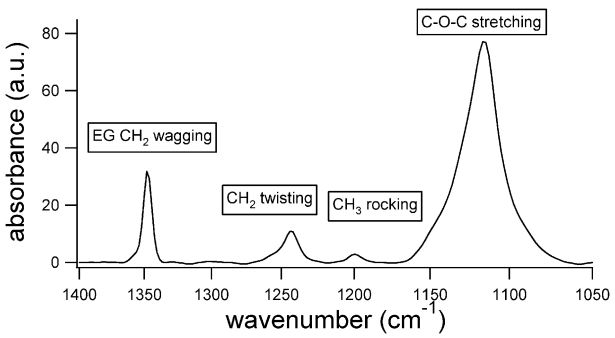

Fig. 1 Spectrum of a fully grown Eg_6OMe SAM under water, one can clearly see the different absorption modes. The dominating feature is the C–O–C stretching mode with its low frequency part at 1115 cm^{-1} and its high frequency part at 1144 cm^{-1}. We can also clearly distinguish the CH_3 rocking peak at 1200 cm^{-1}, the CH_2 twisting peak at 1244 cm^{-1} and the EG CH_2 wagging mode at 1350 cm^{-1}. The dominating low frequency part of the C–O–C stretching mode, the EG CH_2 twisting mode and the strong EG CH_2 wagging mode are indicating a well ordered SAM with predominant helical conformation.

Table 1 Spectral mode assignment of ordered OEG SAMs in helical and all-*trans* conformation respectively (consistent with ref. 9 and 23)

Mode assignment	Eg_6OMe helical/cm^{-1}	Eg_6OMe all-*trans*/cm^{-1}
C–O, C–C stretch (gauge)	1116	
C–O, C–C stretch (*trans*)		1144
CH_3 rock	1200	1200
EG CH_2 twist	1244	
EG CH_2 wag (*trans*)		1325
EG CH_2 wag (gauge)	1348	

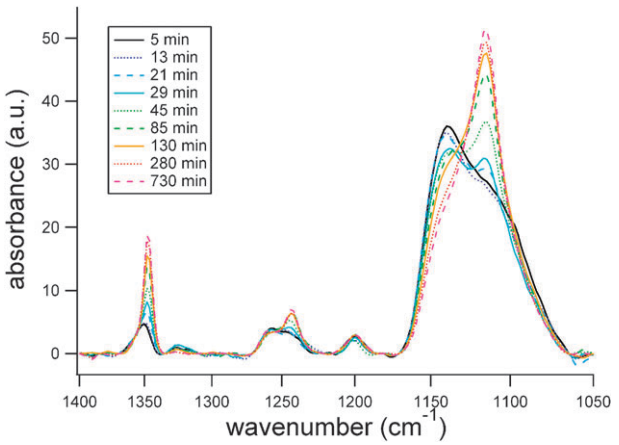

Fig. 2 Spectra of Eg_6OMe in aqueous environment as a function of growth time. The intensity of the low frequency part of the C–O–C stretching mode, the EG CH_2 twisting mode and the EG CH_2 wagging mode are increasing with time, while the intensity of the high frequency part of the C–O–C stretching mode is decreasing. The amplitude of the CH_3 rocking mode is constant.

to an average growth time of 4 minutes, *i.e.* to an intermediate growth state. The data are very stable and reliably monitor subtle changes in the long time ordering process with a superior signal-to-noise ratio, but not the initial growth. With ordering and reordering, respectively, we identify structural and conformational changes of Eg_6OMe thiol molecules after binding to the surface. The time evolution of the absorption spectra is shown in Fig. 2. The position and width of the CH_3 rocking mode (1200 cm^{-1}) is not changing significantly and spreads around its mean value. This is underlining that there is no conformational change of the terminal CH_3 group over the measured time scale. Since there is no detectable intensity change of the CH_3 rocking mode, we assume that the increase of the surface coverage of the SAM is nearly finished until the start of the measurement.

The intensities of the high frequency part of the C–O–C stretching mode at 1145 cm^{-1} and the ether CH_2-wagging mode at 1325 cm^{-1} are decreasing, whereas the intensities of the low frequency part of the C–O–C stretching mode at 1116 cm^{-1}, the ether CH_2-wagging mode at 1350 cm^{-1}, and the CH_2 twisting mode at 1244 cm^{-1} are increasing over the measured period (Fig. 3). The decrease of the modes associated with the all-*trans* conformation and the simultaneous increase of the modes assigned to the helical conformation is indicating an evolution from a mixed helical and all-*trans* conformation to a predominant helical conformation.

In addition to the change in intensity, with progressing time we also find an increasing red shift, as well as a sharpening of the modes. Typical data are shown in Fig. 3. A comparison with spectra of liquid $C_{11}Eg_6OMe$[9] and $C_{11}EG_6OMe$-SAMs grown over night in air reveals that the spectrum of the SAM in early states of our measurement shows more liquid-like features and evolves with time more and more to a spectrum similar to the one in air, suggesting an increasing order over time.

Analysing the time dependence of this ordering process, we find that the increase in intensity as well as the sharpening and the red-shift of the modes follow a single exponential behaviour (Fig. 3). After about 100 min the sharpening of the peaks and the red-shift is finished, whereas the increase in intensity proceeds on a longer timescale.

Besides structural changes there may be also another reason for the decrease of the high frequency part of the C–O–C mode. Malysheva *et al.*[24] calculated infrared spectra for OEG thiols in different orientations. They concluded that even if the conformation is purely helical a high frequency shoulder can occur if the EG moiety is not oriented perpendicular towards the surface.

This is due to the surface selection rule for IRRAS measurements. The part of the electrical field oriented parallel to the surface is eliminated in the vicinity of the surface and so only dipole moments perpendicular to the surface can contribute to the signal. If the EG moiety is oriented perpendicular to the surface only dipole moments which are parallel to the helical axis contribute to the spectrum. However, if the helical axis is tilted, which is suggested in the model of the OEG-SAM in Malysheva *et al.*[25] and which may be also the case at low surface coverage enabling high conformational freedom, also modes perpendicular to the helical axis could contribute to the signal. The position of the strongest mode perpendicular to the helical axis is at 1142 cm^{-1},[24] *i.e.* virtually at the same position as the mode we assign to the C–O–C mode in the all-*trans* conformation.

Since we do not see other modes which are perpendicular to the helical axis and also see a significant shift of the peak positions in the 'fingerprint region' as well as a sharpening, we assumed that orientation effects contribute only marginally to the observed changes in our spectra. This is contrary to the liquid spectrum of OEG, which, of course, shows modes corresponding to all directions.

In order to understand the ordering process better we performed experiments with less concentrated thiol solutions. We noticed that the process slows down, due to its dependence on the thiol concentration, and stopped during the conformational change. Even after waiting over long periods of time (days) the spectrum did not change further. An exchange of the solution against fresh OEG-solution, however led to a further conformational change with an increase of the helical fraction in the SAM. Also we stopped the experiment after a few hours, when the reordering was still in progress, by removing of the OEG-solution and monitored the SAM under pure water. This procedure slows down the ordering process dramatically.

These experiments show that a steady incorporation of thiol molecules is a driving force for the reordering process. If this incorporation stops, the reordering is slowed down

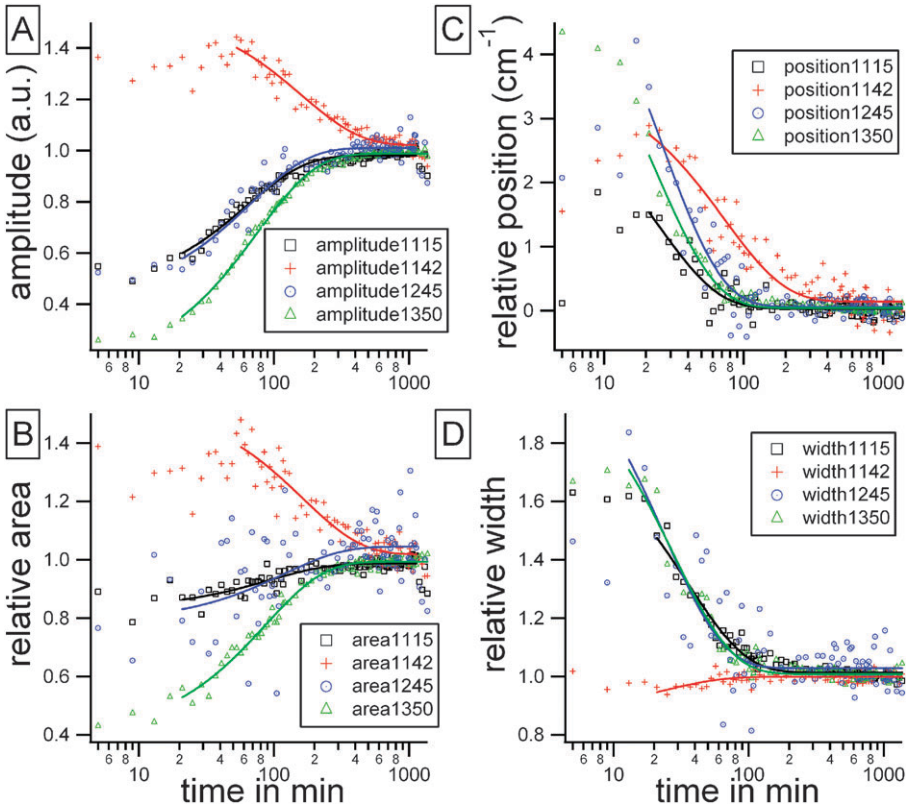

Fig. 3 Kinetic fit of spectral characteristics as a function of time. For visualisation in one graph the values are normalised to the magnitudes at long time. In A and B one can see that amplitude and area of the Gaussian fits of the modes follow an exponential behaviour. While area and amplitude of the modes indicating a helical structure are increasing, the values of the high frequency mode of the C–O–C peak are decreasing indicating an increase in helical structure. In C one can see a red-shift of the peak-positions, towards the positions known for high ordered helical structures. The time scale of the shift of the high-frequency part of the C–O–C mode is significantly slower than the one of the shift of the other modes. In D one can see a sharpening of the peaks of the modes associated with a helical structure, indicating a increase in order over time. The peak of the high frequency mode of the C–O–C peak is not sharpening.

dramatically. This indicates that a dense packing helps to stabilize the energetically favourable helical conformation.

An important point concerning the investigation of SAMs and their properties is their stability over long times. As known from literature,[26,27] OEG thiol SAMs exposed to air and light show substantial changes after a couple of days. To prevent this degeneration it is usual to prepare fresh SAMs directly in advance of experiments.

In order to exclude degeneration effects for our experiments we monitored *in situ* grown SAMs over long times *in situ*. Even after six days we could not find any significant difference in the width, position and intensity of the absorption modes revealing the conformation and crystallinity of the SAM as written above, see ESI.† This indicates that the full-coverage SAM is very stable in solution against degeneration and desorption.

3.3 Interaction with water

In this study the OEG growth is monitored in real-time under aqueous conditions. Therefore we have to take into account the interaction of the SAM with the solvent and the resulting differences of the measured spectra to those obtained in air or vacuum. Skoda *et al.*[17] found a red shift of the C–O–C stretching mode for triethylene glycol-terminated alkanethiol monolayers under aqueous conditions. Also SFG data of the CH_3 region reveal large-scale distortions of the helical structure in liquid environments which leads to an amorphization of the SAM.[14,18] To clarify this point we interrupted the reordering process at different stages and measured spectra of the SAMs in air. By this we were able to compare the corresponding infrared spectra in water and in air.

The spectra measured in air are quite different from the ones measured under aqueous conditions (Fig. 4). At very early growth stages, which we identified by a smaller area of the CH_3 rocking mode indicating a lower surface coverage, the SAM is rather disordered in water as well as in air. At higher coverage, during the reordering process a small area of the EG CH_2 wagging mode and the EG CH_2 twisting mode as well as a broad C–O–C stretching peak with equally high and low frequency components are indicating a poor order. In air the area of the first two modes is much higher and the C–O–C stretching peak is dominated by the low frequency component, indicating a highly ordered helical SAM. A fully grown SAM shows a highly ordered helical conformation whether recorded in air or in solution. Additionally, one can observe a red-shift of the C–O–C peak in water which becomes higher the lower the surface coverage is, compared to Skoda *et al.*[17]

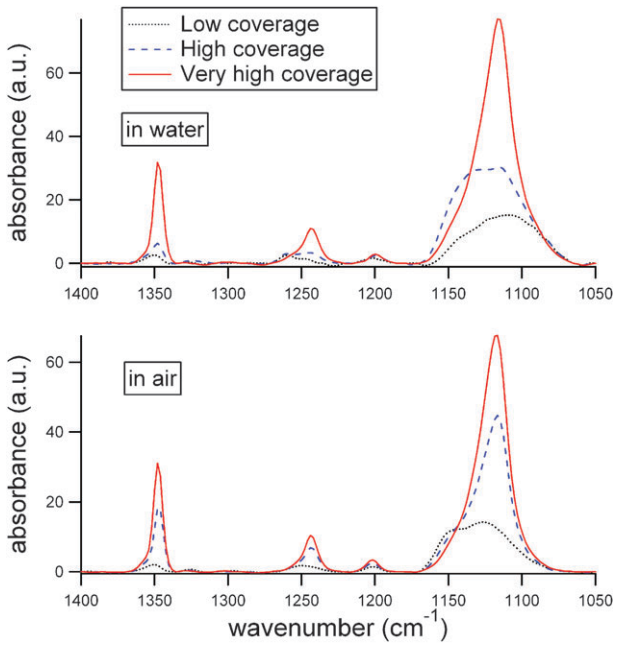

Fig. 4 Spectra of Eg_6OMe SAMs in water at different growth stages and the corresponding spectra in air. At early growth states the SAM shows a low order in air and under water. At intermediate growth stages the ratio of the high frequency part of the C–O–C stretch and the low frequency part is smaller in air, indicating a bigger proportion of molecules in the SAM in helical conformation and therefore a higher order in air. At the end of the growth process the spectra in air as well as in water show high helical order. Note that there is a red shift of the C–O–C peak under water, the earlier the growth state, the higher the shift.

We shall now address the question how these phenomena can be interpreted. The poor order at low surface coverage can be attributed to the high conformational freedom at this stage and the resulting lack of an energetical gain by crystalline packing. With increasing packing density this freedom becomes smaller and a crystalline structure becomes energetically favourable. However, the molecules are not close enough to prevent water molecules from penetrating the SAM and so disturbing the conformation.[14,18] At complete surface coverage the water molecules are no longer able to penetrate the SAM deeply and disturb its structure and so there are only little differences in between the spectra in water and in air. This hypothesis is also supported by the coverage dependence of the red-shift. At low surface coverage there is a strong red-shift in water indicating a strong interaction of the SAM with the solvent, at high coverage and highly ordered SAMs this red-shift nearly vanishes. The larger width of the C–O–C peak at lower surface coverage in water indicates that the different modes contributing to the C–O–C peak are not affected equally by the interaction with water (Fig. 5).[17]

Vanderah *et al.*[12] reported in their studies of protein resistance of OEG-SAMs with different surface coverage that SAMs with complete coverage and perfectly helical structure are not resistant against unspecific protein adsorption while such with lower surface coverage (around 80%) and less well ordered structure are protein resistant. Our measurements suggest that this may be due to the different properties of

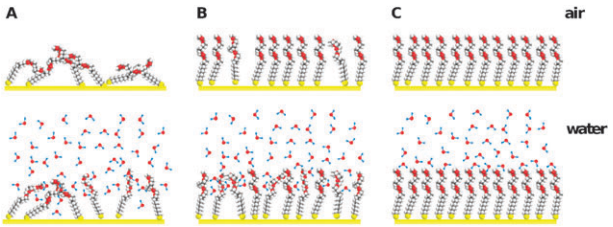

Fig. 5 Schematic of the proposed interaction of water molecules with the Eg_6OMe SAM at different surface coverage. At low surface coverage (A), the ethylene-glycol molecules on the surface are in air as well as under aqueous conditions rather unordered and in amorphous structure, water molecules can easily penetrate the SAM. At high surface coverage (B) the SAM shows a well ordered helical structure in air, however under aqueous conditions water molecules can penetrate deep into the OEG moiety and interact with it, resulting in structural disorder and gauge defects but also in a very stable and energetically favourable structure. For ideally helical SAMs with complete surface coverage (C) the water molecules cannot penetrate the ethylene-glycol moiety and the perfect helical conformation in air is preserved under aqueous conditions.

the SAM to incorporate water molecules dependent of its packing density. Water plays a prominent role in the ability of a SAM to repel proteins[19] and the understanding of the parameters of its interaction with SAMs may lead to a deeper understanding of their protein resistant properties.

4. Conclusions

In this study we have shown that there is a change from a rather amorphous structure with all-*trans* and helical EG conformers to a crystalline structure with helical conformation in the last part of the growth process of a $C_{11}Eg_6OMe$ thiol SAM on gold. This reordering takes place on an exponential time scale. It can be identified by a red-shift as well as a sharpening and an increasing intensity of the vibrational modes associated with a helical conformation. Additionally, the intensities of those modes related to an all-*trans* conformation are decreasing. The lack of a significant change in intensity of the CH_3 rocking peak associated with the CH_3 group adjacent to the water layer above the SAM indicates that the change in surface coverage during the monitored period is small. Nevertheless, we observed that the reordering process is dramatically slowed down if the incorporation of thiols stops.

In addition, we observe that the interaction with water strongly depends on the surface coverage. As can be seen by comparing spectra in air and under aqueous conditions, even for high surface coverage there is a strong penetration of water and interaction with the EG moiety, while a SAM with a full coverage prevents this penetration. Due to these differences it is important to perform *in situ* measurements in order to find out how the SAM behaves in its application under aqueous conditions. Since the ability of the SAM to 'bind' a water layer seems to be crucial for its ability to prevent unspecific protein adsorption, our results are also important to make this property more reproducible.

We showed that *in situ* PMIRRAS measurements are a valuable tool to obtain information about the molecular structure under aqueous conditions. Due to a very thin liquid

layer it is possible to get a high signal-to-noise ratio and so PMIRRAS may be used as a technique complementary to other *in situ* methods for structural investigation like sum frequency generation.

Acknowledgements

We wish to thank M. Skoda and R. Jacobs for fruitful discussions. Also we would like to thank D. Vogel for programming the data analysis software. Funding of N. Martin by the DAAD and support from the Landesstiftung Baden Württemberg is gratefully acknowledged.

References

1 A. Ulman, *Chem. Rev*., 1996, **96**(4), 1533–1554.
2 F. Schreiber, *Prog. Surf. Sci*., 2000, **65**, 151–257.
3 F. Schreiber, *J. Phys.: Condens. Matter*, 2004, **16**(28), R881–R900.
4 K. L. Prime and G. M. Whitesides, *J. Am. Chem. Soc*., 1993, **115**(23), 10714–10721.
5 K. L. Prime and G. M. Whitesides, *Science*, 1991, **252**(5009), 1164–1167.
6 J. Lahiri, L. Isaacs, J. Tien and G. M. Whitesides, *Anal. Chem*., 1999, **71**(4), 777–790.
7 C. Boozer, S. Chen and S. Jiang, *Langmuir*, 2006, **22**(10), 4694–4698.
8 H. Lang, C. Duschl and H. Vogel, *Langmuir*, 1994, **10**(1), 197–210.
9 P. Harder, M. Grunze, R. Dahint, G. M. Whitesides and P. E. Laibinis, *J. Phys. Chem. B*, 1998, **102**(2), 426–436.
10 A. J. Pertsin, M. Grunze and I. A. Garbuzova, *J. Phys. Chem. B*, 1998, **102**(25), 4918–4926.
11 R. Valiokas, M. Ostblom, S. Svedhem, S. C. T. Svensson and B. Liedberg, *J. Phys. Chem. B*, 2000, **104**(32), 7565–7569.
12 D. J. Vanderah, H. La, J. Naff, V. Silin and K. A. Rubinson, *J. Am. Chem. Soc*., 2004, **126**(42), 13639–13641.
13 S. Herrwerth, W. Eck, S. Reinhardt and M. Grunze, *J. Am. Chem. Soc*., 2003, **125**(31), 9359–9366.
14 R. Y. Wang, M. Himmelhaus, J. Fick, S. Herrwerth, W. Eck and M. Grunze, *J. Chem. Phys*., 2005, **122**(16), 164702.
15 R. Valiokas, L. Malysheva, A. Onipko, H.-H. Lee, Z. Ruzele, S. Svedhem, S. C. Svensson, U. Gelius and B. Liedberg, *J. Electron Spectrosc. Relat. Phenom*., 2009, **172**(1–3), 9–20.
16 M. W. A. Skoda, F. Schreiber, R. M. J. Jacobs, J. R. P. Webster, M. Wolff, R. Dahint, D. Schwendel and M. Grunze, *Langmuir*, 2009, **25**(7), 4056–4064.
17 M. W. A. Skoda, R. M. J. Jacobs, J. Willis and F. Schreiber, *Langmuir*, 2007, **23**(3), 970–974.
18 M. Zolk, F. Eisert, J. Pipper, S. Herrwerth, W. Eck, M. Buck and M. Grunze, *Langmuir*, 2000, **16**(14), 5849–5852.
19 R. L. C. Wang, H. J. Kreuzer and M. Grunze, *Phys. Chem. Chem. Phys*., 2000, **2**(16), 3613–3622.
20 I. E. Dunlop, S. Zorn, G. Richter, V. Srot, M. Kelsch, P. A. van Aken, M. Skoda, A. Gerlach, J. P. Spatz and F. Schreiber, *Thin Solid Films*, 2009, **517**(6), 2048–2054.
21 M. Skoda, R. Jacobs, S. Zorn and F. Schreiber, *J. Electron Spectrosc. Relat. Phenom*., 2009, **172**(1–3), 21–26.
22 M. Kobayashi and M. Sakashita, *J. Chem. Phys*., 1992, **96**(1), 748–760.
23 T. Miyazawa, K. Fukushima and Y. Ideguchi, *J. Chem. Phys*., 1962, **37**(12), 2764–2776.
24 L. Malysheva, Y. Klymenko, A. Onipko, R. Valiokas and B. Liedberg, *Chem. Phys. Lett*., 2003, **370**(3–4), 451–459.
25 L. Malysheva, A. Onipko, R. Valiokas and B. Liedberg, *Appl. Surf. Sci*., 2005, **246**(4), 372–376.
26 M.-T. Lee, C.-C. Hsueh, M. S. Freund and G. S. Ferguson, *Langmuir*, 1998, **14**(22), 6419–6423.
27 M. Cerruti, S. Fissolo, C. Carraro, C. Ricciardi, A. Majumdar and R. Maboudian, *Langmuir*, 2008, **24**(19), 10646–10653.

